Trapping of three-dimensional Holstein polarons by various impurities

Hadi Ebrahimnejad[1] and Mona Berciu[1,2]

[1] *Department of Physics and Astronomy, University of British Columbia, Vancouver, BC, Canada, V6T 1Z1*
[2] *Quantum Matter Institute, University of British Columbia, Vancouver, BC, Canada, V6T 1Z4*

(Dated: March 1, 2013)

We study the bound states of a three-dimensional Holstein polaron near various kinds of single impurities, using the momentum average approximation. We show that the electron-phonon coupling is responsible for a strong renormalization of the impurity potential, resulting in an effective potential with significant retardation effects, which describes essential physics ignored by "instantaneous" approximations. The accuracy of our approximation is gauged by comparison with results from Diagrammatic Monte Carlo for the case of an impurity that modifies the on-site energy of the electron. We also discuss impurities that modify the local strength of the electron-phonon coupling, as well as isotope substitutions that change both the electron-phonon coupling and the phonon frequency, and contrast and highlight the difference between these cases.

PACS numbers: 71.38.-k,71.23.An,72.10.Di

I. INTRODUCTION

The challenge to understand the effects of disorder on the behavior of particles strongly coupled to bosons from their environment is commonly encountered in correlated electron systems. For example, high-T_c cuprates are doped anti-ferromagnetic insulators in which, beside strong coupling to magnons, ARPES measurements have also provided evidence for strong electron-phonon coupling.[1] At the same time, charge carriers moving in the CuO_2 layers are subject to random disorder potentials from the adjacent dopant layers. Substituting only a few percent of the Cu atoms with impurities suppresses superconductivity by localizing the low energy electronic states.[2] Inhomogeneities in the superconducting gap measured in high resolution tunnelling experiments have been attributed to atomic scale disorder in the phonon energy and the electron-phonon coupling strength in these materials.[3] Organic semiconductors are another class of materials where interplay between disorder and electron-phonon coupling is believed to be important in determining their properties, and are currently under active investigation.[4,5]

Although the results we present here are valid for any type of bosons (so long as they can be modelled as dispersionless Einstein modes), for simplicity in the following we restrict our discussion to optical phonons. The result of the interplay between disorder and coupling to such phonons depends on their relative strengths. Disorder that is considered weak for free electrons can be strong enough to localize a polaron, that is the dressed quasiparticle which consists of the electron together with its cloud of phonons, because of its heavy effective mass. On the other hand, whereas in the weak disorder regime electron-phonon coupling hinders the motion of electrons, such coupling actually facilitates the electron mobility in the strongly disordered regime where the Anderson localization prevails.[6]

Certain aspects of this problem have been studied with various approximations, most of which rely on sophisticated non-perturbative methods[7] such as the statistical dynamic mean field theory (DMFT),[8,9] or dynamical coherent potential approximation (DCPA).[10,11] The underlying meaning of these approximations and their accuracy is rather hard to gauge. On the computational side, refined versions of the approximation-free diagrammatic Monte Carlo (DMC) technique[12] and of the continuous quantum Monte Carlo algorithm[13] have recently been applied to the problem of a Holstein polaron near a single impurity. While essentially exact, such calculations require significant computational resources, and cannot be easily generalized to other couplings, for example.

Here, we study the bound state formation for a three-dimensional Holstein polaron in the presence of an impurity, using a generalization of the Momentum Average (MA) approximation to inhomogeneous systems.[14] MA was originally developed to study homogeneous systems with various types of electron-phonon coupling.[15–17] It is a non-perturbative method that sums in a closed-form expression all the self-energy diagrams up to exponentially small corrections that are neglected. The method can be systematically improved,[18] therefore providing a fast yet accurate way to scan a vast range of parameters. The method can be used to study all possible types of disorder for various types of electron-phonon coupling. Here, we use it to consider different types of disorder due to single impurities, namely a variation in the on-site energy, in the electron-phonon coupling and/or in the phonon energy are separately considered. The accuracy of this method is demonstrated for the former case by comparison with available DMC results.

Unlike most other theoretical approximations, MA has the important benefit that its structure reveals the essential physics of such problems. It is well-known that electron-phonon coupling leads to the dressing of the particle, resulting in a polaron with a larger effective mass. What MA reveals is that the electron-phonon coupling is also responsible for a *renormalization of the disorder potential*. This renormalization can be very large and has strong retardation effects. Moreover, the renormalized

potential can have a finite-range even if the bare disorder is on-site only. The single impurity problem provides us with a simple test case to understand the effects of this renormalization, and to accurately compare and contrast the behavior of the polaron in the presence of various types of local disorder. Such results are a necessary first step in order to gain the intuition needed for understanding the behavior of more complicated systems.

The paper is organized as follows: In Section II we describe our method and discuss its meaning (full details are provided in the Appendix). Section III presents our results for the three types of impurities, and Section IV contains the summary.

II. MOMENTUM AVERAGE APPROXIMATION FOR INHOMOGENEOUS SYSTEMS

For completeness, we present the MA formalism for the general case of random on-site disorder plus inhomogeneities in both the coupling and the phonon frequencies. A simpler case (with only on-site disorder) has been briefly discussed in Ref. 14. The Hamiltonian is:

$$\mathcal{H} = \mathcal{H}_d + \hat{V}_{el-ph} = \mathcal{H}_0 + \hat{V}_d + \hat{V}_{el-ph}, \tag{1}$$

where $\mathcal{H}_d$ describes the non-interacting part of the Hamiltonian, and for convenience is further divided into:

$$\mathcal{H}_0 = -t\sum_{\langle i,j\rangle}(c_i^\dagger c_j + h.c.) + \sum_i \Omega_i b_i^\dagger b_i$$

which contains the kinetic energy of the particle and the energy of the boson modes ($\hbar = 1$), plus

$$\hat{V}_d = \sum_i \epsilon_i c_i^\dagger c_i$$

describing the on-site disorder. The interaction part:

$$\hat{V}_{el-ph} = \sum_i g_i c_i^\dagger c_i (b_i^\dagger + b_i)$$

describes the (possibly inhomogeneous) Holstein-like coupling[19] between the particle and the bosons. Here, i indexes lattice sites – the lattice can be in any dimension, and of finite or infinite extent. The operators c_i and b_i describe, respectively, particle and boson annihilation from the corresponding state associated with lattice site i. The spin of the particle is ignored because it is irrelevant in this case, but generalizations are straightforward.[20] For simplicity, we assume nearest-neighbour hopping; this approximation can also be trivially relaxed. Depending on the model of interest, the on-site energies ϵ_i, electron-phonon couplings g_i and phonon frequencies Ω_i can be assumed to be random variables. As detailed below, our results here will focus on single on-site impurities such as $\epsilon_i = -U\delta_{i,0}$, but the formalism applies for any model consistent with Eq. (1).

Our goal is to calculate the single polaron Green's function in real space:

$$G_{ij}(\omega) = \langle 0|c_i\hat{G}(\omega)c_j^\dagger|0\rangle = \sum_\alpha \frac{\langle 0|c_i|\alpha\rangle\langle\alpha|c_j^\dagger|0\rangle}{\omega - E_\alpha + i\eta}, \tag{2}$$

where $|0\rangle$ is the vacuum, $\hat{G}(\omega) = [\omega - \mathcal{H} + i\eta]^{-1}$ is the resolvent with $\eta \to 0_+$, and E_α, $|\alpha\rangle$ are single polaron eigenenergies and eigenstates of the Hamiltonian, $\mathcal{H}|\alpha\rangle = E_\alpha|\alpha\rangle$. Knowledge of this Green's function allows us to find the spectrum from the poles, and the local density of states (LDOS) measured in scanning tunneling microscopy (STM) experiments, $\rho(i;\omega) = -\frac{1}{\pi}\mathrm{Im}G_{ii}(\omega)$.

To calculate this quantity, we use repeatedly Dyson's identity: $\hat{G}(\omega) = \hat{G}^d(\omega) + \hat{G}(\omega)\hat{V}_{el-ph}\hat{G}^d(\omega)$, where $\hat{G}^d(\omega) = [\omega - \mathcal{H}_d + i\eta]^{-1}$ is the resolvent for the non-interacting system. The first equation of motion generated this way reads:

$$G_{ij}(\omega) = G^d_{ij}(\omega) + \sum_l g_l F^{(1)}_{il}(\omega)G^d_{lj}(\omega). \tag{3}$$

where

$$G^d_{ij}(\omega) = \langle 0|c_i\hat{G}_d(\omega)c_j^\dagger|0\rangle \tag{4}$$

are, in principle, known quantities and we have introduced the generalized Green's functions:

$$F^{(n)}_{ij}(\omega) = \langle 0|c_i\hat{G}(\omega)c_j^\dagger b_j^{\dagger n}|0\rangle.$$

Note that $F^{(0)}_{ij}(\omega) = G_{ij}(\omega)$. Next, we generate equations of motion for these generalized Green's functions. For any $n \geq 1$, we find:

$$\begin{aligned} F^{(n)}_{ij}(\omega) = &\sum_{l\neq j} g_l G^d_{lj}(\omega - n\Omega_j)\langle 0|c_i G(\omega)c_l^\dagger b_l^\dagger b_j^{\dagger n}|0\rangle \\ &+ g_j G^d_{jj}(\omega - n\Omega_j)\left[F^{(n+1)}_{ij}(\omega) + nF^{(n-1)}_{ij}(\omega)\right] \end{aligned} \tag{5}$$

This equation relates $F^{(n)}$ not only to other Green's functions of a similar type, but also introduces new propagators with phonons at two different sites. Equations of motions can be calculated for these new generalized Green's functions, linking them to yet more general Green's functions, and so on and so forth. The resulting hierarchy of coupled equations describes the problem exactly, but is unmanageable. Approximations are needed to simplify it and find a closed-form solution.

The main idea behind the MA approximations is to simplify this set of equations by neglecting exponentially small contributions in each equation of motion. At the simplest level – the so-called MA$^{(0)}$ approximation – we ignore the first term in Eq. (5) for any $n \geq 1$. This is reasonable at low-energies like the ground state (GS), $\omega \sim E_{GS}$, where $\omega - n\Omega_j$ is well below the energy spectrum of $\mathcal{H}_d$ and, therefore, $G^d_{lj}(\omega - n\Omega_j)$ is guaranteed to decrease exponentially with increasing distance $|l - j|$.

As a result, here we keep the largest $l = j$ propagator, and ignore exponentially smaller $l \neq j$ contributions. Although this is the simplest possible such approximation, it is already accurate at low energies, as shown in the results section. It can also be systematically improved, as discussed below. First, however, we complete this MA$^{(0)}$-level solution.

The simplified equation of motion now reads:

$$F_{ij}^{(n)}(\omega) = g_j G_{jj}^d(\omega - n\Omega_j)\left[F_{ij}^{(n+1)}(\omega) + nF_{ij}^{(n-1)}(\omega)\right].$$

On physical grounds, we know that $F_{ij}^{(n)}(\omega)$ must vanish for sufficiently large n, because its Fourier transform is the amplitude of probability that a particle injected in the system will generate n phonons in time t, and this must vanish for large enough n. As a result, these recursive equations admit the solution:

$$F_{ij}^{(n)}(\omega) = A_n(j,\omega)F_{ij}^{(n-1)}(\omega),$$

where the continued-fraction:

$$A_n(j,\omega) = \frac{ng_j G_{jj}^d(\omega - n\Omega_j)}{1 - g_j G_{jj}^d(\omega - n\Omega_j)A_{n+1}(j,\omega)} \qquad (6)$$

can be efficiently evaluated starting from a cutoff $A_{N_c}(j,\omega) = 0$ for a sufficiently large N_c. Generally speaking, this cutoff N_c must be much larger than the average number of phonons expected at site j; in practice, the cutoff is increased until convergence is reached to within the desired accuracy. Substituting $F_{ij}^{(1)}(\omega) = A_1(j,\omega)G_{ij}(\omega)$ in Eq. (3) leads to a closed system of linear equations for the original Green's function:

$$G_{ij}(\omega) = G_{ij}^d(\omega) + \sum_l G_{il}(\omega)g_l A_1(l,\omega)G_{lj}^d(\omega). \qquad (7)$$

This equation has a similar structure to the equation linking the disorder Green's function to the free particle propagator $G_{ij}^{(0)}(\omega) = \langle 0|c_i[\omega + i\eta - \mathcal{H}_0]^{-1}c_j^\dagger|0\rangle$ (in the absence of coupling to phonons), which is depicted diagrammatically in Fig. 1(a), and which reads:

$$G_{ij}^d(\omega) = G_{ij}^{(0)}(\omega) + \sum_l G_{il}^d(\omega)\epsilon_l G_{lj}^{(0)}(\omega). \qquad (8)$$

This analogy shows that coupling to phonons renormalizes the on-site disorder $\epsilon_l \to \epsilon_l + g_l A_1(l,\omega)$. Note that $A_1(l,\omega)$ depends not only on the local phonon frequency Ω_l and coupling g_l, but also on *all* the bare on-site energies ϵ_i through the disorder propagators G^d. This is the simplest example of the emergence of a renormalized potential for this problem, that is made very transparent within the MA approximation.

While Eq. (7) can be solved directly for a finite-size system, we can improve its efficiency and reveal a different physical interpretation by explicitly removing the "average" contribution due to the electron-phonon interactions. Let g and Ω be the average values of the g_i, Ω_i distributions. We assume that the on-site energy average $\epsilon = 0$ (a finite value results in a trivial shift of all energies). Then, let:

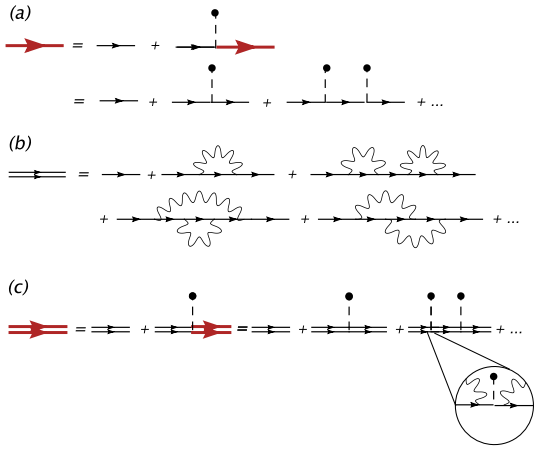

FIG. 1. (color online) Diagrammatic expansion for (a) the disorder Green's function $G_{ij}^d(\omega)$ (bold red line); (b) the polaron Green's function in a clean system $G_{ij}^{(0)}(\tilde{\omega})$ (double thin line), and (c) the "instantaneous" approximation for the polaron Green's function in a disordered system, $G_{ij}^d(\tilde{\omega})$ (double bold red line). The thin black lines depict free electron propagators, the wriggly lines correspond to phonons, and scattering on the disorder potential is depicted the dashed lines ending with circles. See text for more details.

$$A_n(\omega) = \frac{ngg_0(\omega - n\Omega)}{1 - gg_0(\omega - n\Omega)A_{n+1}(\omega)} \qquad (9)$$

be the continued fractions corresponding to these average parameters, where we use the short-hand notation:

$$g_0(\omega) = G_{ii}^{(0)}(\omega) = \frac{1}{N}\sum_{\mathbf{k}} \frac{1}{\omega - \epsilon_{\mathbf{k}} + i\eta}$$

for the on-site free propagator (in the absence of disorder, this quantity becomes independent of the site). It is given by the momentum average of the free propagator, where ϵ_k is the free-particle dispersion.

The "average" renormalization of the on-site energy is now recognized to represent the corresponding MA$^{(0)}$ self-energy for a "clean" system, i.e. a homogeneous system with average coupling and phonon frequency:

$$\Sigma_{\mathrm{MA}^{(0)}}(\omega) = gA_1(\omega)$$

see, for instance, Eqs. (11) and (12) of Ref. 18.

Introducing the effective disorder potential:

$$v_0(l,\omega) = g_l A_1(l,\omega) - \Sigma_{\mathrm{MA}^{(0)}}(\omega), \qquad (10)$$

Eq. (7) can be rewritten as:

$$G_{ij}(\omega) = G_{ij}^d(\tilde{\omega}) + \sum_l G_{il}(\omega)v_0(l,\omega)G_{lj}^d(\tilde{\omega}), \qquad (11)$$

where $\tilde{\omega} = \omega - \Sigma_{\mathrm{MA}^{(0)}}(\omega)$. This energy renormalization, $\omega \to \tilde{\omega}$, reflects the fact that processes describing the formation of the polaron in the "clean" system have been explicitly summed.

Besides being numerically more efficient, since now $v_0(j,\omega)$ contains only the fluctuations from the (not necessarily small) average value included in $\tilde{\omega}$, Eq. (10) reveals a different interpretation for the effects of the interplay between disorder and electron-phonon coupling.

Consider first the meaning of $G^d_{ij}(\tilde{\omega})$, which would be the solution if we could ignore $v_0(j,\omega)$. In the absence of on-site disorder this term equals $G^{(0)}_{ij}(\tilde{\omega})$, i.e. the expected solution for a polaron in the clean system, depicted diagrammatically in Fig. 1(b) (of course, the exact self-energy is here approximated by $\Sigma_{\mathrm{MA}^{(0)}}(\omega)$). Comparing Figs. 1(a) and 1(b), it follows that $G^d_{ij}(\tilde{\omega})$ is the sum of the diagrams shown in Fig. 1(c).

At first sight, this seems to be the full answer for this problem, since these diagrams sum the contributions of all the processes in which the polaron scatters once, twice, etc., on the disorder potential. This is certainly the answer obtained in the limit of an "instantaneous" approximation valid when $\Omega \to \infty$, i.e. when the ions are very light and respond instantaneously to the motion of electrons. In this case, one can perform a Lang-Firsov transformation and after an additional averaging over phonons, one obtains an approximative effective Hamiltonian:[13,21]

$$\mathcal{H}_{inst} = -t^* \sum_{\langle i,j \rangle} (c_i^\dagger c_j + h.c.) + \sum_i \left(\epsilon_i - \frac{g^2}{\Omega} \right) c_i^\dagger c_i \quad (12)$$

where $t^* = te^{\frac{-g^2}{\Omega^2}}$ is the renormalized polaron hopping, and $-g^2/\Omega$ is the polaron formation energy (for simplicity, here we assume that the phonon energies and electron-phonon coupling are homogeneous, $g_i \to g, \Omega_i \to \Omega$). The Green's function of this Hamiltonian is also given by Fig. 1(c), if the polaron propagator is approximated by:

$$G^{(0)}_{ij}(\tilde{\omega}) \to \frac{1}{N} \sum_{\mathbf{k}} \frac{e^{i\mathbf{k}\cdot(\mathbf{R_i}-\mathbf{R_j})}}{\omega - \epsilon^*_{\mathbf{k}} + \frac{g^2}{\Omega} + i\eta}$$

where $\epsilon^*_{\mathbf{k}}$ is the renormalized kinetic energy. Of course, using the full expression of $G^{(0)}_{ij}(\tilde{\omega})$ is preferable since the self-energy $\Sigma_{\mathrm{MA}^{(0)}}(\omega)$ describes much more accurately the overall energy shift and effective mass renormalization than those asymptotic expressions, besides also including the quasiparticle weight.

That $G^d_{ij}(\tilde{\omega})$ cannot be the full answer becomes obvious if we consider what happens when we rewrite the clean polaron propagators in terms of free particle and phonon lines, i.e. we substitute the expansion of Fig. 1(b) in 1(c). Doing so reveals that within this "instantaneous" approximation, scattering of the electron on the disorder potential is allowed only when no phonons are present, see zoom-in in Fig. 1(c). However, we know that for moderate and large electron-phonon coupling, the probability to find no phonons in the system is exponentially small, therefore the processes summed in Fig. 1(c) have very low probabilities.

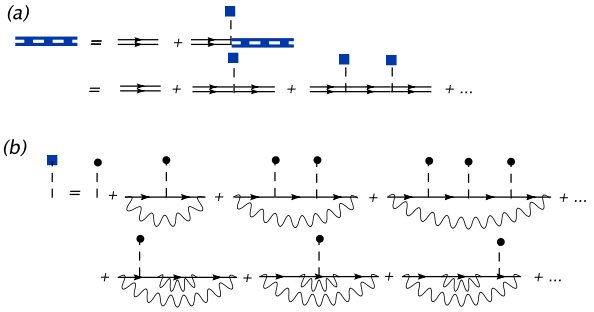

FIG. 2. (color online) (a) Diagrammatic expansion for the full MA solution $G_{ij}(\omega)$ (thick dashed blue line) in terms of the clean polaron Green's function (double thin line) and scattering on the renormalized disorder potential $\epsilon^*_l(\omega)$, depicted by dashed lines ended with squares. (b) Diagrammatic expansion of $\epsilon^*_l(\omega)$. For more details, see text.

What is missing in Fig. 1(c) are diagrams describing the scattering of the electron on the disorder potential in the presence of the phonons from the polaron cloud. Their contribution is included through the renormalized potential $v_0(l,\omega)$ in the second term of Eq. (11). Indeed, the full MA solution shows that the polaron scatters not on the bare disorder ϵ_l, but on the renormalized disorder potential

$$\epsilon^*_l(\omega) = \epsilon_l + v_0(l,\omega), \quad (13)$$

as depicted in Fig. 2(a). The diagrammatic expansion of the additional term $v_0(l,\omega)$, shown in Fig. 2(b), verifies that it indeed describes the effective scattering in the presence of arbitrary numbers of phonons.

Taken together, the diagrams summed in Fig. 2 represent all possible contributions to the polaron propagator in the disordered system. The $\mathrm{MA}^{(0)}$ approximation consists in discarding exponentially small contributions from each of these diagram, as already discussed. $\mathrm{MA}^{(0)}$ also has an exact variational meaning, namely of assuming that the polaron cloud can have phonons only on a single site, in direct analogy with the clean case.[18,22] It is quite remarkable that all the diagrams corresponding to this variational approximation can still be summed analytically in closed form, even in the presence of disorder.

As is the case for the clean system, MA can be systematically improved by keeping more contributions to Eq. (5). In particular, at the $\mathrm{MA}^{(1)}$ level, we also treat the equation for the $F^{(1)}$ functions exactly, and make the MA approximation of discarding exponentially small off-diagonal propagators only for $n \geq 2$. The logic here is that the propagators appearing in $F^{(1)}$ have the highest energy, therefore the slowest exponential decay. The $\mathrm{MA}^{(1)}$ equations can also be solved in closed form. The details are presented in the Appendix. The final solution

looks identical to Eq. (11), except the renormalized energy is now $\tilde{\omega} = \omega - \Sigma_{\mathrm{MA}^{(1)}}(\omega)$ while the renormalized potential $v_0(l,\omega)$ is replaced by a more complicated, yet more accurate expression $v_1(l,\omega)$. The meaning of all these quantities, however, is the same.

To summarize, MA reveals that the role of electron-phonon coupling is two-fold. On one hand, it renormalizes the quasiparticle properties due to polaron formation, just like in a clean system (as revealed by the explicit appearance of the "clean" system self-energy). However, this coupling also renormalizes the disorder potential experienced by the particle, $\epsilon_l \to \epsilon_l^*(\omega)$. As we show next for various types of disorder, this renormalization is non-trivial in that it has strong retardation effects, and has significant consequences. "Instantaneous" approximations completely ignore this renormalization, and therefore miss essential physics. To be fair, in practice the "instantaneous" approximations are usually implemented in an improved, variational form[21,23] which is certain to be much more accurate. However, this leads to the necessity to calculate the variational parameters through a self-consistent loop, making the improved version computationally as complicated as DMFT and DCPA, which also have self-consistency loops.

In contrast, MA gives a closed analytical expression for all quantities of interest, in a formulation whose meaning is very transparent, and whose accuracy can be systematically improved.

III. POLARON NEAR A SINGLE IMPURITY

We now apply the general formalism described above to the simplest type of "disorder", namely an otherwise clean 3D simple cubic lattice with a single impurity. Impurities which modulate the on-site energy, the strength of the electron-phonon coupling and/or the phonon frequency are separately considered. We investigate under what conditions such impurities can trap the polaron.

As a reference case, we first review here briefly the solution in the absence of electron-phonon coupling. In this case, the impurity can only modulate the on-site potential, $\epsilon_i = -U\delta_{i,0}$, and the Hamiltonian reduces to:

$$\mathcal{H}_{\mathrm{d}} = -t \sum_{<ij>} (c_i^\dagger c_j + h.c.) - U c_0^\dagger c_0 = \mathcal{H}_0 + \hat{V}_d. \quad (14)$$

For this form of $\hat{V}_d$, Eq. (8) reads:

$$G_{ij}^d(\omega) = G_{ij}^{(0)}(\omega) - U G_{i0}^d(\omega) G_{0j}^{(0)}(\omega), \quad (15)$$

and is trivially solved to find:

$$G_{ij}^d(\omega) = G_{ij}^{(0)}(\omega) - U \frac{G_{i0}^{(0)}(\omega) G_{0j}^{(0)}(\omega)}{1 + U G_{00}^{(0)}(\omega)}. \quad (16)$$

Of course, because of translational and time reversal symmetry, $G_{ij}^{(0)}(\omega) = G_{i-j,0}^{(0)}(\omega) = G_{j-i,0}^{(0)}(\omega)$, etc.

The LDOS at the impurity site is then found to be:

$$\rho(0;\omega) = -\frac{1}{\pi}\mathrm{Im}G_{00}^d(\omega) = \frac{\rho_0(0;\omega)}{|1 + U G_{00}^{(0)}(\omega)|^2},$$

where $\rho_0(0;\omega) = -\frac{1}{\pi}\mathrm{Im}G_{00}^{(0)}(\omega)$ is the LDOS in the clean system (equal to the DOS, because of translational invariance). As a result, a bound state below the continuum, signalled by a delta-function peak in $\rho(0;\omega)$, occurs if and only if the denominator of Eq. (16) vanishes. For a 3D simple cubic lattice this means that an impurity bound state appears if there is an energy $E < -6t$ such that $\mathrm{Re}G_{00}^{(0)}(E) = -1/U$ (below the continuum the imaginary part of $G_{00}^{(0)}(E)$ vanishes). This equation can be solved graphically to find that a bound state appears for any $U \geq U_c = -\frac{1}{\mathrm{Re}G_{00}^{(0)}(-6t)} \sim 3.96t$.

In the presence of electron-phonon coupling the equations are more complicated, but the idea is the same: we calculate the LDOS at the impurity site and compare it to the DOS of the clean system. If the former has a peak below the threshold of the latter, then a bound state exists at that energy. We then vary U to find the critical value above which a bound state is guaranteed. More details about the impurity state, such as its localization length, statistics for the phonon cloud, etc., can be extracted from the LDOS at sites in the neighbourhood of the impurity. Here we focus on identifying when bound impurity states are stable.

A. Impurity changing the on-site energy

The Hamiltonian describing this case is:

$$\mathcal{H} = \hat{T} + \Omega \sum_i b_i^\dagger b_i + g \sum_i c_i^\dagger c_i (b_i + b_i^\dagger) - U c_0^\dagger c_0, \quad (17)$$

where $\hat{T}$ is the electron's tight-binding Hamiltonian. We are interested in the attractive impurities, $U > 0$, when an impurity state can be bound near the impurity site. To find the LDOS at the impurity site, we need to solve Eq. (11) to find $G_{00}(\omega)$. Note that now $G_{ij}^d(\omega)$ is known, being given by Eq. (16). The free-particle propagators $G_{ij}^{(0)}(\omega) = \frac{1}{N}\sum_{\mathbf{k}} \frac{e^{i\mathbf{k}\cdot(\mathbf{R_i}-\mathbf{R_j})}}{\omega - \epsilon_{\mathbf{k}} + i\eta}$, where for the simple cubic lattice $\epsilon_{\mathbf{k}} = -2t\sum_{i=1}^3 \cos k_i$, can be calculated by doing the integrals over the Brillouin zone. A more efficient approach, which we use, is discussed in Ref. 24.

In this case, the renormalized impurity potential decays fast at sites away from the impurity, because $G_{ll}^d(\omega) \to G_{ll}^{(0)}(\omega)$ when $|l| \to \infty$, so that $A_1(l,\omega) \to A_1(\omega)$. Physically, this is because the impurity has less and less influence at sites far from where it is located. Mathematically, this follows from Eq. (16) and the fact that $G_{l0}^{(0)}(\omega)$ decreases exponentially with the distance between site l and the origin, at energies below the free particle continuum, of interest here. As a result, in Eq.

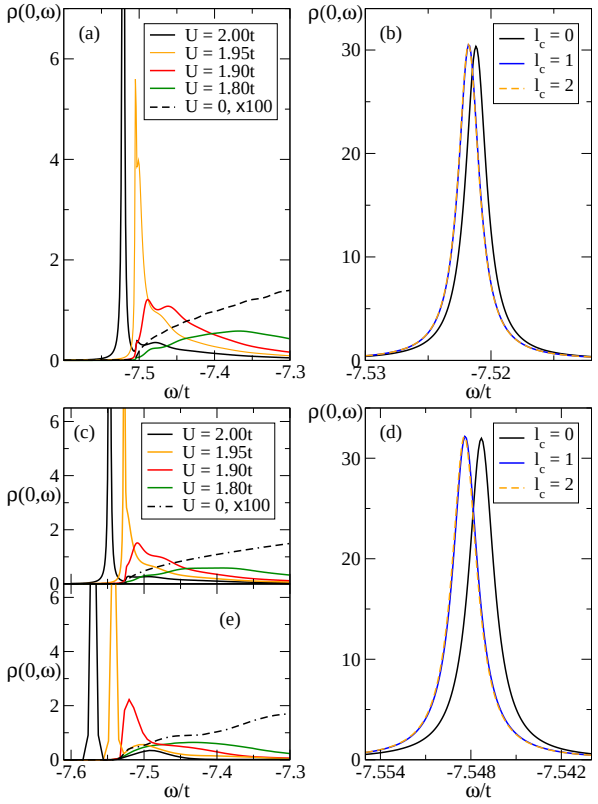

FIG. 3. (color online) LDOS at the impurity site $\rho(0,\omega)$ in units of $1/t$, vs. the energy ω/t, for (a) MA$^{(0)}$ with $l_c = 0$ for $U = 1.8, 1.9, 1.95$ and 2.0. The dashed line shows the DOS for the clean system, times 100; (b) MA$^{(0)}$ at $U/t = 2$, and cutoffs in the renormalized potential $l_c = 0, 1, 2$. Panels (c) and (d) are the same as (a) and (b), respectively, but using MA$^{(1)}$. Panel (e) shows DMC results from Ref. 12, for same parameters as (a) and (b). Other parameters are $\Omega = 2t, \lambda = 0.8, \eta/t = 10^{-3}$.

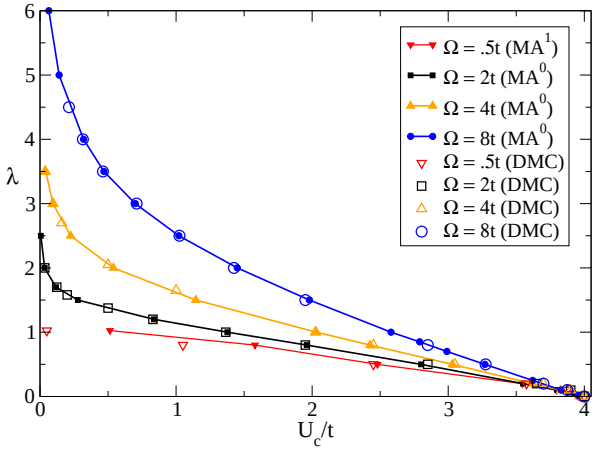

FIG. 4. (color online) Phase diagram separating the regime where the polaron is mobile (below the line) and trapped (above the line). The effective coupling is $\lambda = g^2/(6t\Omega)$, and the critical trapping potential U_c is shown for several values of Ω/t. The MA results (filled symbols) compare well with the DMC results of Ref. 12 (empty symbols).

(11) we only need to sum over sites l close to the impurity, and the system can be solved very efficiently.

The appropriate value for this cutoff varies depending on the various parameters, but generically it decreases as the energies of interest become lower. Again, mathematically this is due to the exponential decrease of the free particle propagator with distance, and the fact that this decrease becomes faster as $\omega \to -\infty$. Physically, this can be understood as follows. First, let us explain why is the renormalized disorder potential non-local, even though the bare impurity potential is local. The answer is provided by the diagrams which contribute to it, see Fig. 2(b). Consider, for simplicity, the MA$^{(0)}$ approximation. In this case, all phonon lines appearing in these diagrams start and end at the site l for which $v_0(l,\omega)$ is being calculated – this is the site where the phonon cloud is located. However, the electron is found with various probabilities away from the polaron cloud, so it can scatter on the impurity if this is located within the "radius" of the polaron, where the electron resides. In other words, the range of the renormalized potential is controlled by the polaron size. From medium to large couplings, as the polaron becomes smaller, the renormalized potential becomes more local. At small couplings, though, the distance between the electron and its phonon cloud can be appreciable, and the range of the potential increases.

In Fig. 3(a) we plot $\rho(0,\omega)$ over a wider energy range, for several values of U, within MA$^{(0)}$. The dashed line shows the DOS of the clean system, multiplied by 100 for visibility. For $U/t = 1.8, 1.9$, the impurity attraction is not sufficient to bind a state below the continuum, although the LDOS is pushed towards the lower band-edge. For $U = 1.95t$, there is a peak just below the continuum. Because of the finite value of η, the two features are not completely separated and the continuum onset looks like a "shoulder", however lowering η allows us to clearly separate the two features (not shown). Finally, for $U = 2t$ the bound state peak is clearly below the continuum, so in this case $U_c \approx 1.95t$. This U_c value equals that obtained in DMC, although our energies are overall higher than the exact DMC values shown in Fig. 3(e), as expected for a variational approximation. At the MA$^{(1)}$ level the agreement with DMC is significantly improved since all features move toward lower energies, see Fig. 3(c). The critical value $U_c \approx 1.95t$ at which an impurity state appears below the continuum is little affected, however, by this overall shift of the spectral weights.

The dependence of the bound state energy on the cutoff is shown in Figs. 3(b) and (d) for MA$^{(0)}$ and MA$^{(1)}$, respectively, for the case with $U = 2t$, $\Omega = 2t$ and the effective coupling $\lambda = \frac{g^2}{6t\Omega} = 0.8$. At these energies, keeping only the local part in MA$^{(0)}$, i.e. setting $v_0(l,\omega) \to \delta_{l,0} v_0(l,\omega)$, is already a very good approximation. Including the correction from the 6 nearest neighbor sites ($l_c = 1$) lowers the energy somewhat, but the contribution from the second nearest neighbor sites ($l_c = 2$)

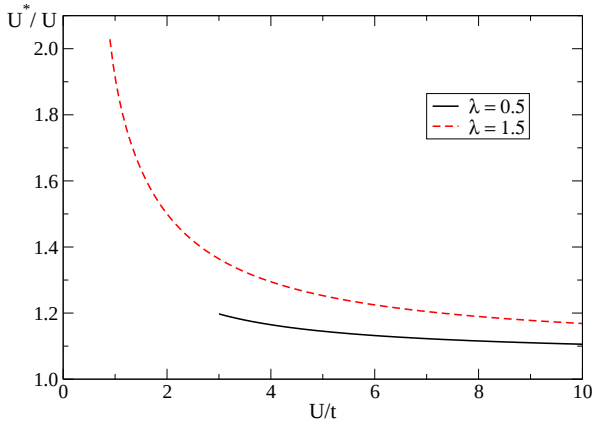

FIG. 5. (color online) Effective value of the impurity attraction U^*/U, extracted from the scaling $E_B^*/t^* = f(U^*/t^*)$, for $\lambda = 0.5, 1.5$ and $\Omega = 3t$. In order to have the best fit to the data, we plot each curve starting from slightly larger U/t than the corresponding U_c/t given in Fig. (4). For more details, see text.

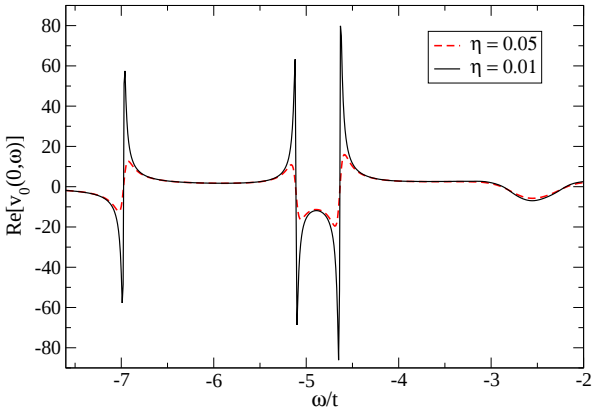

FIG. 6. (color online) Real part of the additional on-site MA$^{(0)}$ disorder potential $v_0(0,\omega)$ over a wide energy range, for $U = 2t, \Omega = 2t, \lambda = 0.8$ and two values of η.

is no longer visible on this scale for either the MA$^{(0)}$ or the MA$^{(1)}$ results.

Repeating this process for other values of the parameters, we trace U_c in the parameter space. This is shown in Fig. 4, for $\Omega/t = 0.5, 2, 4, 8$ and various effective couplings. The MA results (filled symbols) are in good quantitative agreement with the DMC results (empty symbols) for larger $\Omega \geq 1$ values (these are MA$^{(0)}$ results for cutoff $l_c = 0$. Using MA$^{(1)}$ and/or increasing the cutoff changes the values of U_c by less than 1% everywhere we checked). For the smaller frequencies such as $\Omega = 0.5t$, MA is known to become quantitatively less accurate at intermediary couplings[15,18], and indeed, here we see a discrepancy with the DMC data even for the MA$^{(1)}$ results. To improve the quantitative agreement here, one should use a 2- or 3-site MA variational approximation for the phonon cloud, as discussed in Refs. 17.

As expected, when $\lambda \to 0$, U_c goes towards the expected critical value in the absence of electron-phonon coupling, of roughly $3.96t$. As the effective coupling increases U_c decreases, but the lines never intersect the y-axis: $U_c = 0$ is impossible, since the polaron cannot be trapped (localized) in a clean system as long as it has a finite effective mass, i.e. for any finite value of λ.

The decrease of U_c with increasing λ is expected, and is usually attributed to the fact that the effective polaron mass increases with λ, and this makes it easier to trap near the impurity.[12] However, we claim that this is not the full story, and that the renormalization of the trapping potential also plays a non-trivial role.

Consider, first, the Hamiltonian of Eq. (14), which describes the impurity problem in the absence of electron phonon coupling. The binding energy of the impurity state (once formed) is a monotonic function of the only dimensionless parameter of this problem: $\frac{E_B}{t} = f\left(\frac{U}{t}\right)$ for any $\frac{U}{t} \geq \frac{U_c}{t} \approx 3.96$. If one views the polaron as a quasiparticle with an effective hopping t^* which scatters on the same potential U as the bare particle (instantaneous approximation), then the polaron binding energy should be $\frac{E_B^*}{t^*} = f\left(\frac{U}{t^*}\right)$ for any $\frac{U}{t^*} \geq \frac{U_c}{t^*} \approx 3.96$. In particular, this predicts $U_c/t = 3.96t^*/t$ decreasing with increasing λ, in qualitative agreement with Fig. 4.

This hypothesis can be tested. The function $f(x)$ is easy to calculate numerically, we can extract the binding energy E_B^* for the trapped states by comparing their trapped energy to the GS energy of the polaron in the clean system, and the effective hopping $t^* \sim 1/m^*$ is directly linked to the effective polaron mass m^* in the clean system.[15] We find that this scaling is not obeyed. Instead, one needs to also rescale the impurity potential, i.e. use $\frac{E_B^*}{t^*} = f\left(\frac{U^*}{t^*}\right)$ where $U^* \neq U$. Of course, this scaling assumes that the scattering potential is local. As we discussed, this is not true although it is a good approximation for medium and large couplings.

In Fig. 5 we show the renormalized value U^*/U extracted this way, as a function of U/t above the corresponding threshold values U_c/t, for a medium and a large effective coupling $\lambda = 0.5, 1.5$ and $\Omega = 3t$. Qualitatively similar curves are found for other parameters. We see that $U^* \to U$ only when $U \to \infty$ and becomes the dominant energy scale (hence anything else is a small perturbation). For fixed U, Ω, we find that U^* increases with increasing coupling λ – this is also expected, since the renormalization is directly caused by the electron-phonon coupling, see Fig. 2(b).

This renormalization is a direct illustration of the general result of Eq. (13): the electron-phonon coupling changes not only the properties of the polaron (its effective mass), but also the disorder potential it experiences.

However, it is very wrong to expect that the potential renormalization can always be described by a simple rescaling by some overall value. Indeed, Eq. (13) shows that the renormalized potential is expected to be a function of energy, because of retardation effects. This

function is not roughly constant, instead it has significant and very non-trivial dependence of ω, as illustrated by plotting $v_0(0,\omega)$ over a large energy range, in Fig. 6. Similar curves are found for other values of the parameters. Over a narrow range of energies around $\omega \sim -7.5t$ where the bound state forms for these parameters (see Fig. 3), $v_0(0,\omega)$ varies slowly and can be approximated as an overall negative constant. This explains why here we can approximate $\epsilon_0^*(\omega) = -U + v_0(0,\omega) \approx -U^*$, with $U^* > U$, as discussed above. At higher energies, however, $v_0(0,\omega)$ goes through singularities and changes sign from negative to positive and back. Although at first sight these singularities are surprising, they should be expected based on Eq. (10). The self-energy of the Holstein polaron is known to have such singularities, especially at medium and higher couplings where an additional second bound state forms and the continuum above shows strong resonances spaced by Ω. In particular, as $\lambda \to \infty$ and the spectrum evolves towards the discrete Lang-Firsov limit $E_n = -\frac{g^2}{\Omega} + n\Omega$, the self-energy has a singularity at the top of each corresponding band. The renormalized potential of Eq. (10) is the difference between two such curves, displaced from each other. It is thus not a surprise that it has such nontrivial behavior.

Physically, such strong retardation effects are not surprising, either, since the additional potential $v_0(i,\omega)$ describes the scattering of the electron in the presence of the phonon cloud. The structure of the phonon cloud varies with energy, for instance one expects quite different clouds within the polaron band vs. at higher energies, in the continuum of incoherent states with finite lifetime. This suggests that the diagrams of Fig. 2(b) that contribute most to the series change with energy, and so does the total result. As a final note, we mention that at these higher energies, MA$^{(1)}$ should be used. It is well-known that MA$^{(0)}$ fails to describe properly the location of the polaron+one phonon continuum, since it does not include the needed variational states.[22] This problem is fixed at the MA$^{(1)}$ and higher levels.[18]

To summarize, for this simple impurity problem the MA approximation is found to agree well with results from DMC in describing the trapping of the polaron. Although quantitatively not as accurate, besides efficiency its main advantage is that the analytic equations that describe MA allow us to understand the relevant physics. In particular, we showed that coupling to bosons renormalizes the disorder in a very non-trivial way.

B. Impurity changing the electron-phonon coupling

We now assume that the impurity does not change the on-site energy, but instead it modifies the value of electron-phonon coupling at its site:

$$\mathcal{H} = \hat{T} + \Omega \sum_j b_j^\dagger b_j + \sum_j g_j c_j^\dagger c_j (b_j + b_j^\dagger), \qquad (18)$$

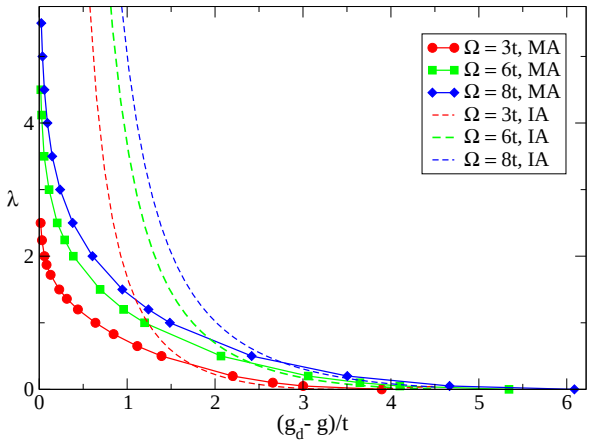

FIG. 7. (color online) Phase diagram separating the regime where the polaron is delocalized (below the line) and trapped (above the line), as a function of the difference between the impurity and the bulk electron-phonon coupling, $g_d - g$. Symbols show MA$^{(0)}$ results, while the dashed black lines correspond to the instantaneous approximation.

where $g_j = g + (g_d - g)\delta_{j0}$. Thus, g_d and g are the electron-phonon couplings at the impurity site and in the bulk of the system, respectively. Since $\hat{V}_d = 0$ in this case, the non-interacting part of the Hamiltonian is $\mathcal{H}_d = \mathcal{H}_0$. Thus, $G_{jj}^d(\omega - n\Omega) \to G_{jj}^{(0)}(\omega - n\Omega) \equiv g_0(\omega - n\Omega)$ in the continued fractions, Eq. (6), whose dependance on the site index j is now through the coupling g_j only. As a result, the effective disorder potential $v_0(j,\omega)$ vanishes everywhere except at the impurity site, $j = 0$:

$$v_0(j,\omega) \equiv \Delta(\omega)\delta_{j0}, \qquad (19)$$

where $\Delta(\omega) = g_d A_1(0,\omega) - g A_1(\omega)$, and $A_1(0,\omega)$ is like in Eq. (9) but with $g \to g_d$. This shows that even though $\epsilon_i = 0$ in this case, the inhomogeneity gives rise to an effective potential $\epsilon_i^*(\omega) = \delta_{i,0}\Delta(\omega)$. This is now local because only when the phonon cloud is at the impurity site it can experience the different coupling.

Equation (11) can now be solved analytically to find:

$$\rho(0,\omega) = -\frac{1}{\pi}\mathrm{Im}\left(\frac{g_0(\tilde{\omega})}{1 - \Delta(\omega)g_0(\tilde{\omega})}\right). \qquad (20)$$

We now find the critical values $g_d - g$ when an impurity state emerges below the continuum, for given values of g, Ω. The results are shown in Fig. 7 for $g_d > g$, when the polaron formation energy at the impurity site, $-g_d^2/\Omega$, is lower than the bulk value $-g^2/\Omega$, and a bound state may be expected to form even within the instantaneous approximation. Symbols show MA$^{(0)}$ results, while the dashed lines are for the instantaneous approximation. The two agree quantitatively only in the limit $\lambda \to 0$. This proves that the additional renormalization included in MA is significant for this type of impurity, as well. We note that all critical lines intercept the x-axis at a finite value, *i.e.* for any value of Ω and $g = 0$, there is a critical

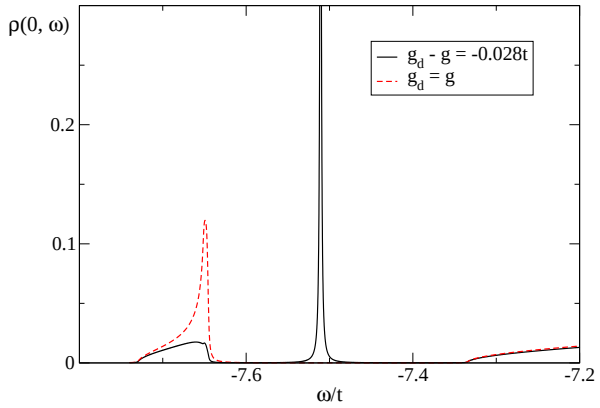

FIG. 8. For large λ, in the clean system (dashed red line) the first polaron band is separated by an energy gap from the next features in the spectrum (here, the band associated with the second bound state). For $g_d < g$, an "anti-bound" impurity state is pushed inside this gap (black full line). Parameters are $\Omega = t = 1$, $\lambda = 1.2$ and $\eta = 10^{-3}$.

finite value g_d above which an impurity state forms. For example, for $\Omega = 3t$ this critical value is $g_d \approx 3.9t$. Its value increases with increasing Ω, as expected.

Unlike for an impurity which changes the on-site potential, and which can bind at most one impurity state, impurities which change the electron-phonon coupling can bind multiple impurity levels. As g_d increases and the energy of the impurity level moves towards lower energies, additional bound states, spaced by roughly Ω, emerge whenever the distance between the last one and the bulk polaron band is of order Ω.

The origin of this sequence of bound states is straightforward to understand in the limit $g_d \gg g, t$, where, the Hamiltonian is, to zero order:

$$\mathcal{H} \approx g_d c_0^\dagger c_0 (b_0^\dagger + b_0) + \Omega b_0^\dagger b_0,$$

with $c_0^\dagger c_0 \approx 1$ because the weight of the bound state is concentrated at the impurity site. This Hamiltonian can be exactly diagonalized with the Lang-Firsov transformation[25] and predicts a series of equally spaced eigenenergies $n\Omega - g_d^2/\Omega$. For finite t, g, all states which lie below the bulk polaron continuum become impurity states, and basically describe excited bound states with additional phonons at the impurity site.

So far we have considered $g_d > g$, where a ground-state impurity level can emerge. It is important to note that discrete peaks can also appear for $g_d < g$, although not at low energies. This happens when λ is sufficiently large that there is a gap between the bulk polaron band and higher features in the spectrum, such as the polaron+one phonon continuum, or the band associated with the second bound state, once it forms.[26] A typical example is shown in Fig. 8, where in the presence of an impurity with a weaker coupling $g_d < g$ (full line), a discrete state appears above the polaron band. Since most of its weight is removed from the bulk polaron band (dashed line), we interpret this as being an "anti-bound" polaron state. A similar state is also expected to appear for a repulsive on-site $U < 0$ potential.

C. Isotope impurity

The last case we consider in detail is an isotope impurity. Because of its different mass $M_d \neq M$, both its phonon frequency $\Omega_d \sim M_d^{-\frac{1}{2}}$, and its electron-phonon coupling $g_d \propto 1/\sqrt{M_d \Omega_d} \sim M_d^{-\frac{1}{4}}$, are changed. Interestingly, both the effective coupling $\lambda_d = g_d^2/(6t\Omega_d) = g^2/(6t\Omega) = \lambda$ and the polaron formation energy $-g_d^2/\Omega_d = -g^2/\Omega$ show no isotope effect.[27] As a result, within the instantaneous approximation of Eq. (12) one would predict that the isotope is "invisible" and the polaron spectrum is basically unaffected by its presence.

We consider a single isotope impurity located at the origin:

$$\mathcal{H} = \hat{T} + \sum_j g_j c_j^\dagger c_j (b_j + b_j^\dagger) + \sum_j \Omega_j b_j^\dagger b_j, \qquad (21)$$

where $\Omega_j = \Omega + (\Omega_d - \Omega)\delta_{j0}$ and $g_j = g + (g_d - g)\delta_{j0}$ are chosen such that $\lambda_d = \lambda$.

Just like in the previous section, because there is no on-site disorder $\epsilon_i = 0$, we have $G^d_{jj}(\omega) = G^{(0)}_{jj}(\omega)$ and the effective disorder potential is again local, *i.e.* it vanishes everywhere but at the impurity site. As a result, the LDOS at the impurity site is given by Eq. (20), except that here:

$$\Delta(\omega) = \Sigma_d(\omega) - \Sigma_{\mathrm{MA}^{(0)}}(\omega), \qquad (22)$$

where $\Sigma_d(\omega)$ has the same functional form like $\Sigma_{\mathrm{MA}^{(0)}}(\omega)$, but with $g \to g_d, \Omega \to \Omega_d$.

From investigations of this LDOS at different parameters we find that there exists a threshold value of the effective coupling, λ^*, below which low-energy bound states do not form irrespective of how small or large M_d/M is. In other words, for $\lambda < \lambda^*$, the behavior agrees with the prediction of the instantaneous approximation.

We can estimate a bound on λ^* as follows. Consider the case of a very light isotope, so that $\Omega_d, g_d \gg \Omega, g, t$. In this limit, $\Sigma_d(\omega) \to -g_d^2/\Omega_d = -6t\lambda$. The bound state appears when the LDOS is singular because its denominator vanishes:

$$1 - \Delta(\omega) g_0(\tilde{\omega}) = 0 \to \Sigma_{\mathrm{MA}^{(0)}}(\omega) + 1/g_0(\tilde{\omega}) = -6t\lambda, \qquad (23)$$

after using Eq. (22) and $\Sigma_d(\omega) \approx -6t\lambda$.

Consider now the limiting case when a bound state emerges just below the bulk polaron ground state, *i.e.* Eq. (23) has a solution at $\omega \leq \varepsilon_{gs}^{pol}$. In the clean system, the polaron ground-state energy ε_{gs}^{pol} is the lowest pole of $G(k = 0, \omega) = [\omega - \epsilon_{\mathbf{k}=0} - \Sigma_{\mathrm{MA}^{(0)}}(\omega)]^{-1}$, so it satisfies: $\varepsilon_{gs}^{pol} = -6t + \Sigma_{\mathrm{MA}^{(0)}}(\varepsilon_{gs}^{pol})$. Using this in Eq. (23) suggests

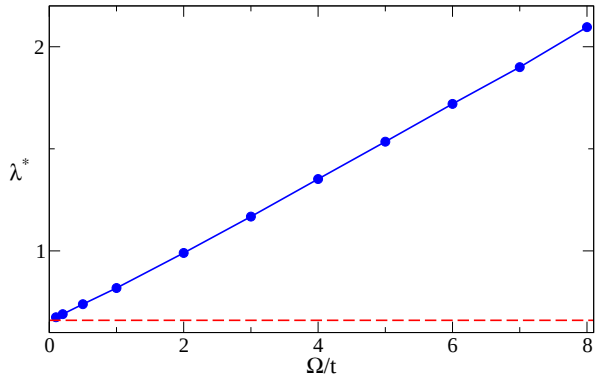

FIG. 9. (color online) Critical effective coupling λ^* above which an impurity state may appear for a sufficiently light isotope. Below this line, polarons cannot be bound near isotopes. Symbols shows $\mathrm{MA}^{(0)}$ results. The dashed line is the analytic low-bound for λ^* discussed in the text.

that a solution can exist if $\lambda > \lambda^*$, where

$$\lambda^* = \left|\frac{\varepsilon_{gs}^{pol}}{6t}\right| - 1 - \frac{1}{6tg_0(-6t)}, \qquad (24)$$

with $g_0(-6t) \approx -1/3.96t$. Since $\varepsilon_{gs}^{pol} \to -6t$ as $\lambda \to 0$, we expect that $\lambda^* \to 0.66$ in this limit, and that it increases as ε_{gs}^{pol} becomes more negative, for example with increasing λ. These considerations are confirmed by the data shown in Fig. 9. Here, the symbols show values of λ^* found numerically with $\mathrm{MA}^{(0)}$, and the dashed line is the lower bound of 0.66, discussed above.

For $\lambda > \lambda^*$, bound impurity states can appear near isotopes if g_d and $\Omega_d = g_d^2/(6t\lambda)$ are sufficiently large. In Fig. 10 we show critical lines for two cases, $\Omega = 4t, 8t$. The symbols show the $\mathrm{MA}^{(0)}$ results, which converge towards their corresponding λ^* values as $\Omega_d \to \infty$, as expected. Of course, the largest values considered for Ω_d are unphysical; we use them only to illustrate the convergence towards λ^*.

The existence of a region of the parameter space where bound polaron states appear near an isotope is in direct contradiction of the instantaneous approximation, and again illustrates the importance of the renormalized disorder potential $\Delta(\omega)$ which makes their trapping possible. In this context, it is worth mentioning that there is clear evidence for electronic states bound near isotope O^{16} defects in CuO_2 planes,[28] although the precise nature of these states has not been clarified and the measurements are certainly not in the extremely underdoped regime where our single-polaron results are valid.

Interestingly, when such bound states form near an isotope, the spectrum is different than that for the other two types of impurities. As shown in Fig. 11, bound states now appear simultaneously both below and above the bulk polaron continuum, not just below it. This provides a possible "fingerprint" for polarons trapped near isotopes. Finally, we note that even when no low-energy impurity state is observed, it is again possible to have higher energy bound states inside the gaps opening between various features in the bulk polaron spectrum.

To summarize, in the presence of isotope defects, polarons in the weakly coupled regime $\lambda < \lambda^*$ always remain delocalized. Only for $\lambda > \lambda^*$ it is possible to trap polarons near an isotope. This makes this case quite distinct from the other two cases, where bound states exist for any λ if the impurity is strong enough.

IV. SUMMARY AND CONCLUSIONS

We studied the threshold for the emergence of polaron bound states near various types of single impurities, using the momentum-average approximation. Electron-phonon coupling was shown to strongly renormalize the impurity potential in a nontrivial way which includes strong retardation effects. This is a feature that is completely absent in the instantaneous approximation, which is the only other available "simple" description of this problem.

We considered the simplest models of impurities that change the strength of the on-site energy, the local electron-phonon coupling, or are isotope substitutions that modify both the coupling and the phonon energy. We calculated the polaron binding phase diagrams for each case. The first case had been considered previously by numerical methods,[12,13] and our results are in good quantitative agreement with their predictions. To our knowledge, the other two cases have not been investigated before. We showed that in the first two cases bound states always exist for a sufficiently strong impurity, however the polaron remains delocalized for the case of isotope substitution of arbitrary strength if the effective coupling is weaker than a threshold value, λ^*. Differences in the LDOS at the impurity site have also been found, such as the possibility to bind multiple states

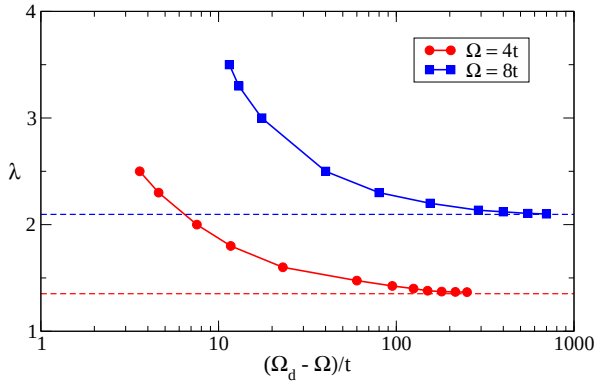

FIG. 10. (color online) Phase diagram separating the regime where the polaron is delocalized (below the line) and trapped (above the line), as a function of the difference between the $\Omega_d - \Omega$, on a logarithmic scale. Symbols show $\mathrm{MA}^{(0)}$ results for $\Omega = 4t, 8t$. As $\Omega_d \to \infty$, these critical lines converge towards their corresponding λ^* (dashed lines), below which polaron states are always delocalized.

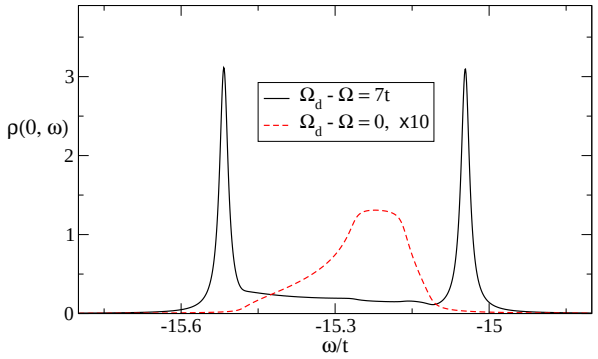

FIG. 11. (color online) LDOS at the impurity site near an isotope with $\Omega_d = \Omega + 7t$ (full line). Two discrete states, one above and one below the bulk polaron band, are seen. For comparison, the DOS in the clean system (multiplied by 10) is shown as a dashed line. Parameters are $\Omega = 4t$, $\lambda = 2.5$ and $\eta = 10^{-2}$.

near an impurity that changes the coupling, or the unusual fingerprint of discrete states both below and above the bulk polaron continuum, for an isotope bound state.

Of course, a realistic description of an impurity in a real system may combine several of these inhomogeneities, and even the form of the electron-phonon coupling could be affected. MA gives an efficient yet quite accurate way to deal with such cases, and can be easily generalized to other types of couplings where MA has been used succesfully to describe bulk properties.

Whereas we expect the single impurity results to remain valid for a system with multiple impurities if the mean free path is long and the polaron interacts with one impurity at a time, in the presence of significant disorder, when multiple scattering processes become important, the polarons can undergo Anderson localization. This limit has been addressed within a generalized DMFT,[8] however we believe that our simpler formulation might provided additional insight and uncover previously unexplored aspects of Anderson localization for polarons. Such work is currently in progress.

ACKNOWLEDGMENTS

We thank Andrey Mishchenko and Holger Fehske for useful discussions and sharing their results. This work was supported by NSERC and CIFAR.

Appendix A: IMA$^{(1)}$

At the IMA$^{(1)}$ level, one also allows processes in which one phonon is away from the phonon cloud. These are described by the propagators $S_n(i,l,j;\omega) = \langle 0|c_i G(\omega) c_l^\dagger b_l^{\dagger n-1} b_j^\dagger|0\rangle$ with $j \neq l$. In terms of these, Eq. (3) can be written as

$$G_{ij}(\omega) = G^d_{ij}(\omega) + \sum_l g_l S_1(i,l,l;\omega) G^d_{lj}(\omega). \tag{A1}$$

Once again we apply the Dyson identity to S_1

$$\begin{aligned} S_1(i,l,j;\omega) &= g_j G^d_{jl}(\omega-\Omega_j) G_{ij}(\omega) \\ &\quad + \sum_m g_m G^d_{ml}(\omega-\Omega_j) S_2(i,m,j;\omega). \end{aligned} \tag{A2}$$

This exact equation relates S_1 to the propagators S_2. We can similarly find the equation of motion of all higher, $n \geq 2$, $S_n(i,l,j;\omega)$ with $l \neq j$ and $l = j$, separately. For $l \neq j$ we have

$$\begin{aligned} S_n(i,l,j;\omega) &= g_l G^d_{ll}(\omega-(n-1)\Omega_l-\Omega_j) \\ &\quad \times[(n-1)S_{n-1}(i,l,j;\omega) + S_{n+1}(i,l,j;\omega)], \end{aligned} \tag{A3}$$

where we now ignore contributions from terms with a second phonon away from the polaron cloud, as they are exponentially smaller than those we kept. This admits the solution $S_n(i,l,j;\omega) = B_n(l,j;\omega) S_{n-1}(i,l,j;\omega)$, where

$$\begin{aligned} B_n(l,j;\omega) &= \frac{(n-1) g_l G^d_{ll}(\omega-(n-1)\Omega_l-\Omega_j)}{1 - g_l G^d_{ll}(\omega-(n-1)\Omega_l-\Omega_j) B_{n+1}(l,j;\omega)} \\ &= A_{n-1}(l,\omega-\Omega_j). \end{aligned} \tag{A4}$$

For $l = j$ and $n \geq 2$, $S_n(i,l,l;\omega) = F^{(n)}_{il}(\omega)$ and we get the same solution as in MA$^{(0)}$, i.e. $S_n(i,l,l;\omega) = A_n(l,\omega) S_{n-1}(i,l,l;\omega)$. The relations between S_2 and S_1 are used in Eq. (A2) to turn it into an equation between $S_1(\omega)$ and $G_{ij}(\omega)$ only

$$\begin{aligned} S_1(i,l,j;\omega) &= g_j G^d_{jl}(\omega-\Omega_j) G_{ij}(\omega) \\ &\quad + g_j G^d_{jl}(\omega-\Omega_j) A_2(j,\omega) S_1(i,j,j;\omega) \\ &\quad + \sum_{m\neq j} g_m G^d_{ml}(\omega-\Omega_j) A_1(m,\omega-\Omega_j) S_1(i,m,j;\omega). \end{aligned}$$

Together with Eq. (A1), this can be solved to find $G_{ij}(\omega)$. However, it is again convenient to explicitly extract the "average" contributions, to make these equations more efficient.

We therefore remove the homogeneous part from Eq. (A2) and include it into a renormalized energy:

$$S_1(i,l,j;\omega) = g_j G^d_{jl}(\bar\omega_j)[G_{ij}(\omega) + (A_2(j,\omega) - A_1(j,\omega-\Omega_j))S_1(i,j,j;\omega)] + \sum_{m\neq j} g_m G^d_{ml}(\bar\omega_j)[A_1(m,\omega-\Omega_j) - A_1(\omega-\Omega)]S_1(i,m,j;\omega). \quad \text{(A5)}$$

where $\bar\omega_j = \omega - \Omega_j - gA_1(\omega-\Omega)$, and $A_1(\omega-\Omega)$ is given by Eq. (9) for the "average" clean system.

The sum on the rhs of Eq. (A5) again convergences for a very small cutoff, only sites m very close to j need to be included. Its general solution is of the form:

$$S_1(i,l,j;\omega) = x_{jl}(\omega)[G_{ij}(\omega) + (A_2(j,\omega) - A_1(j,\omega-\Omega_j))S_1(i,j,j;\omega)], \quad \text{(A6)}$$

where

$$x_{jl}(\omega) = g_j G^d_{jl}(\bar\omega_j) + \sum_{m\neq j} g_m G^d_{ml}(\bar\omega_j)[A_1(m,\omega-\Omega_j) - A_1(\omega-\Omega)]x_{jm}(\omega).$$

In fact, using $x_{jl}(\omega) = g_j G^d_{jl}(\bar\omega_j)$ is already a very good approximation, since the terms in the sum are exponentially small – but one can go beyond this. Once $x_{jj}(\omega)$ is known, from Eq. (A6) we find $S_1(i,j,j,\omega) = \Lambda_j(\omega)G_{ij}(\omega)$, where

$$\Lambda_j(\omega) = \frac{x_{jj}(\omega)}{1 - x_{jj}(\omega)\,(A_2(j,\omega) - A_1(j,\omega-\Omega_j))}.$$

This can now be used in Eq. (A1) to turn it into an equation for $G_{ij}(\omega)$ only:

$$G_{ij}(\omega) = G^d_{ij}(\omega) + \sum_l g_l \Lambda_l(\omega) G_{il}(\omega) G^d_{lj}(\omega). \quad \text{(A7)}$$

As we did in Eq. (11) for MA$^{(0)}$, this can be made efficient to solve by subtracting the MA$^{(1)}$ self-energy and including it into the energy argument

$$G_{ij}(\omega) = G^d_{ij}(\tilde\omega) + \sum_l G_{il}(\omega) v_1(l,\omega) G^d_{lj}(\tilde\omega), \quad \text{(A8)}$$

in which $\tilde\omega = \omega - \Sigma_{\mathrm{MA}^{(1)}}(\omega)$ and $v_1(l,\omega) = g_l\Lambda_l(\omega) - \Sigma_{\mathrm{MA}^{(1)}}(\omega)$. Here, $\Sigma_{\mathrm{MA}^{(1)}}(\omega)$ is the value of $g_l\Lambda_l(\omega)$ in the clean, "average" system:

$$\Sigma_{\mathrm{MA}^{(1)}}(\omega) = \frac{g^2 g_0(\bar\omega)}{1 - g g_0(\bar\omega)\,(A_2(\omega) - A_1(\omega-\Omega))}$$

where now $\bar\omega = \omega - \Omega - gA_1(\omega-\Omega)$.[18] This completes the calculation of Green's function within inhomogeneous MA$^{(1)}$ approximation.

[1] A. Lanzara, P. V. Bogdanov, X. J. Zhou, S. A. Kellar, D. L. Feng, E. D. Lu, T. Yoshida, H. Eisaki, A. Fujimori, K. Kishio, J. -I. Shimoyama, T. Noda *et al.*, Nature **412**, 510 (2001).

[2] D. N. Basov, B. Dabrowski, and T. Timusk, Phys. Rev. Lett. **81**, 2132 (1998).

[3] J. Lee, K. Fujita, K. McElroy, J. A. Slezak, M. Wang, Y. Aiura, H. Bando, M. Ishikado, T. Masui, J.-X. Zhu, A. V. Balatsky, H. Eisaki, S. Uchida *et al.*, Nature **442**, 546 (2006).

[4] H. Matsui, A. S. Mishchenko and T. Hasegawa, Phys. Rev. Lett. **104**, 056602 (2010).

[5] S. Ciuchi and S. Fratini, Phys. Rev. Lett. **106**, 166403 (2011)

[6] S. M. Girvin and M. Jonson, Phys. Rev. B **22**, 3583 (1980).

[7] O. Gunnarsson, M. Calandra, and J. E. Han, Rev. Mod. Phys. **75**, 1085 (2003).

[8] F. X. Bronold, and H. Fehske, Phys. Rev. B **66**, 073102 (2002); F. X. Bronold, A. Alvermann, and H. Fehske, Philos. Mag. **84**, 673 (2004). For LDA, see A. Alvermann and H. Fehske: *Local Distribution Approach*, Lecture Notes in Phys. **739**, 505-526 (Springer, 2008).

[9] S. Ciuchi, F. de Pasquale, S. Fratini, and D. Feinberg, Phys. Rev. B **56**, 4494 (1997).

[10] H. Sumi, J. Phys. Soc. Jpn. **36**, 770 (1974);

[11] F. X. Bronold, A. Saxena and A. R. Bishop, Phys. Rev. B **63**, 235109 (2001).

[12] A. S. Mishchenko, N. Nagaosa, A. Alvermann, H. Fehske, G. De Filippis, V. Cataudella, and O. P. Sushkov, Phys. Rev. B **79**, 180301(R) (2009).

[13] J. P. Hague, P. E. Kornilovitch, and A. S. Alexandrov, Phys. Rev. B **78**, 092302 (2008).

[14] M. Berciu, A. S. Mishchenko and N. Nagaosa, EPL **89**, 37007 (2010).

[15] M. Berciu, Phys. Rev. Lett. **97**, 036402 (2006); G. L. Goodvin, M. Berciu, and G. A. Sawatzky, Phys. Rev. B **74**, 245104 (2006).

[16] G. L. Goodvin and M. Berciu, Phys. Rev. B **78**, 235120 (2008).

[17] M. Berciu and H. Fehske, Phys. Rev. B **82**, 085116 (2010); D. J. J. Marchand, G. De Filippis, V. Cataudella, M. Berciu, N. Nagaosa, N. V. Prokof'ev, A. S. Mishchenko,

and P. C. E. Stamp, Phys. Rev. Lett. **105**, 266605 (2010).
[18] M. Berciu and G. L. Goodvin, Phys. Rev. B **76**, 165109 (2007); M. Berciu, Phys. Rev. Lett. **98**, 209702 (2007).
[19] T. Holstein, Ann. Phys. (N.Y.) **8**, 325 (1959); **8**, 343 (1959).
[20] L. Covaci and M. Berciu, Phys. Rev. Lett. **102**, 186403 (2009).
[21] A.N. Das and S. Sil, Phys. Lett. A **348**,266 (2006); in a somewhat different context, see also A.N. Das and S. Sil. J. Phys.: Condens. Matter **5**, 8265 (1993) or A. Macridin, G. A. Sawatzky and Mark Jarrell, Phys. Rev. B **69**, 245111 (2004).
[22] O. S. Barisic, Phys. Rev. Lett. **98**, 209701 (2007).
[23] M. Hohenadler, H. G. Evertz and W. von der Linden, Phys. Rev. B 69, 024301 (2004).
[24] M. Berciu and A. M. Cook, Europhys. Lett. **92**, 40003 (2010).
[25] I. G. Lang and Y. A. Firsov, Sov. Phys. JETP **16**, 1301 (1963).
[26] J. Bonca, S.A. Trugman, and I. Batistic, Phys. Rev. B **60**, 1633 (1999).
[27] A. S. Mishchenko and N. Nagaosa, Phys. Rev. B **73**, 092502 (2006).
[28] C. Bernhard, T. Holden, A. V. Boris, N. N. Kovaleva, A. V. Pimenov, J. Humlicek, C. Ulrich, C. T. Lin, and J. L. Tallon, Phys. Rev. B **69**, 052502 (2004).